Nonbasel Deformation Modes of HCP Metals and Alloys: Role of Disloction Source and Mobility

Paper Review by Cindy Smith

Yoo, Morris, Ho, and Agnew, Met. and Mat. Trans A, vol 33A, March 2002

Possible HCP slip systems

Table III. Independent Modes of Deformation in hcp Crystals

Direction	Plane	Crystallographic Elements	Number of Independent Mode
	Basal Slip	$(0002)\langle 11\bar{2}0\rangle$	2
a	Prismatic Slip	$\{1\bar{1}00\}\langle 11\bar{2}0\rangle$	2
	Pyramidal Slip	$\{1\bar{1}0l\}\langle 11\bar{2}0\rangle$	4
c		$\{hk\bar{i}0\}[0001]$	
c + a	Pyramidal Slip	$\{hkil\}$*$\langle 11\bar{2}3\rangle$	5
Twinning		$\{K_1\}\langle\bar{\eta}_1\rangle$†	0-5

* See Fig. 1.
† See Table 4.

Zr RT deformation systems are:
- Prismatic slip $\{10\bar{1}0\}<1\bar{2}10>$
- Tension twins $\{10\bar{1}2\}<\bar{1}011>$, and $\{11\bar{2}1\}<\bar{1}\bar{1}26>$
- Compression twin $\{11\bar{2}2\}<\bar{1}\bar{1}23>$

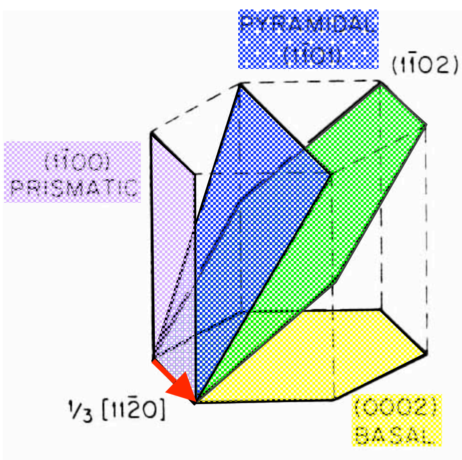

ā SLIP

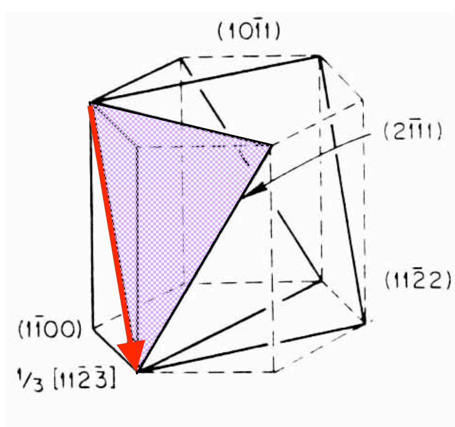

c̄ + ā SLIP

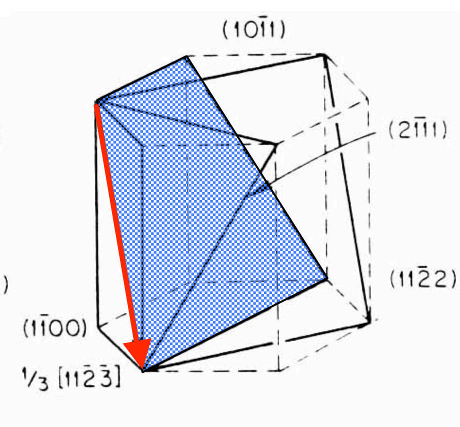

c̄ + ā SLIP

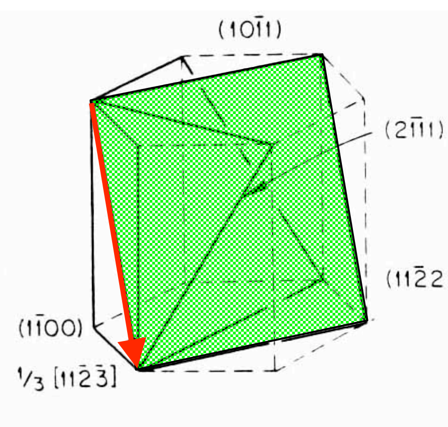

c̄ + ā SLIP

K_1, K_2, η_1, η_2 notation

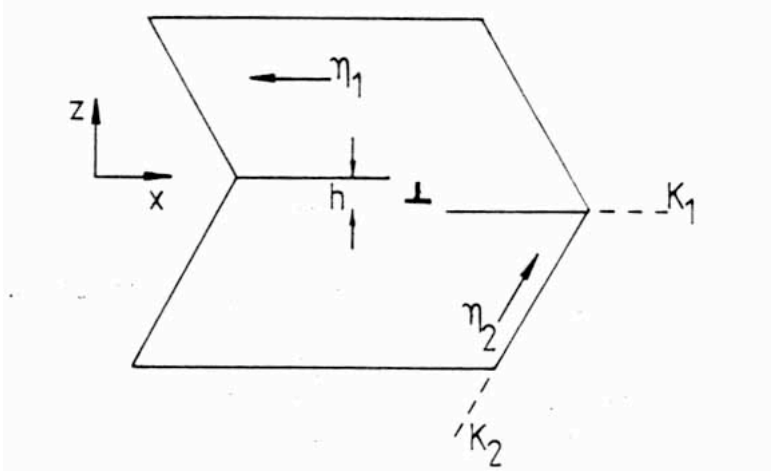

Fig. 1. Schematic illustration of a twinned crystal showing the twinning elements K_1, η_1, K_2 and η_2, and the interfacial step associated with a twinning dislocation.

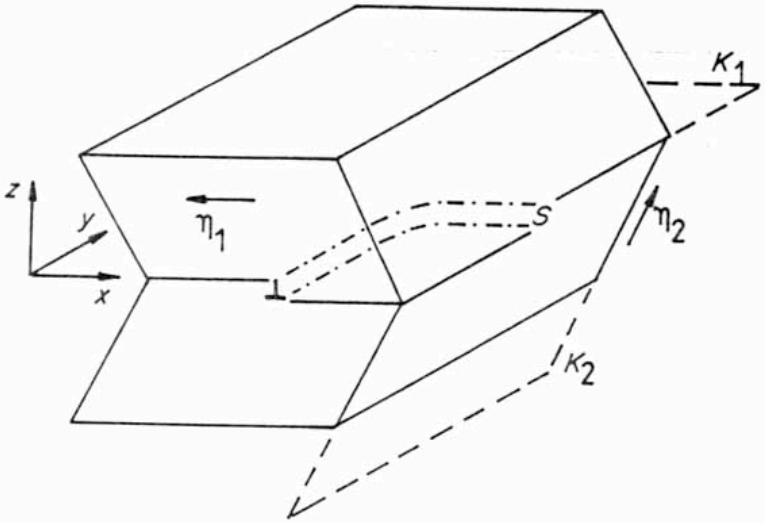

Fig. 4. Schematic illustration of a twinned crystal showing the twinning elements K_1, η_1, K_2 and η_2, and the interfacial step associated with a twinning dislocation (of class 1 or 2).

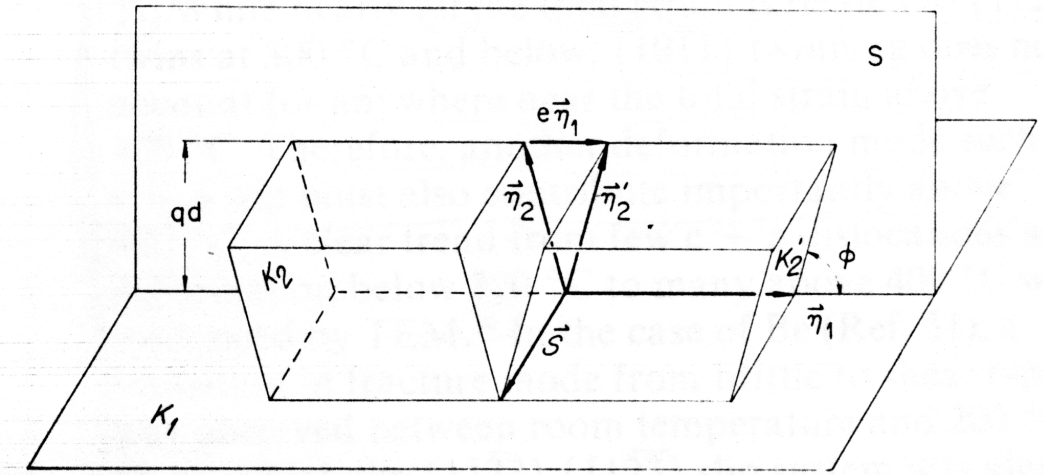

Fig. 3—Crystallographic elements of twinning. The unit cell defined by η_1, η_2, and S is homogeneously sheared to the unit cell in twin defined by η_1, η_2', and S.

K_1 = twinning plane
K_2 = conjugate twinning plane
η_1 = twinning direction
η_2 = conjugate twinning direction
s = twinning shear

Intro

- Due to the diverse behavior of hcp materials, little is understood of the mechanisms of nonbasel modes.
  - Why are particular materials demonstrate particular deformation modes under a given stress?
  - How do the deformation modes depend on Temperature?
- In practice, stress applied along the c axis is usually accomidated by deformation along the <c+a> = <1123> direction.
- The Burgers vector b = <c+a> is large compared to interatomic spacing, suggesting a dissociated configuration and nonplanar core structure
  - This strongly affects the mobility of the dislocations
  - Atomistic simulations verify this.
- There is also a question if the critical resolved shear stress (CRSS) for <c+a> slip depends on dislocation mobility or dislocation source and generation processes.

Outline

- Experimental results of slip vs twinning for various HCP metals
- Twin boundaries and stacking faults role in deformation, experimental observations and energy calculations
- Deformation twin nucleation theories
- Twin growth and propagation theories
- <c+a> pyramidal slip
  - Dislocation source, core structures, and mobility
- Discussion of results for pure HCP metals and for alloys.

Ti Single Crystals

- There was considerable amounts of scatter in the original data, this curve is of the approximate median of the data.
- Below T/Tm = 0.3 is associated with {1122} twinning, and above is <c+a> slip in combination with {1011} twinning.
- Several researchers have reported similar results for Ti.

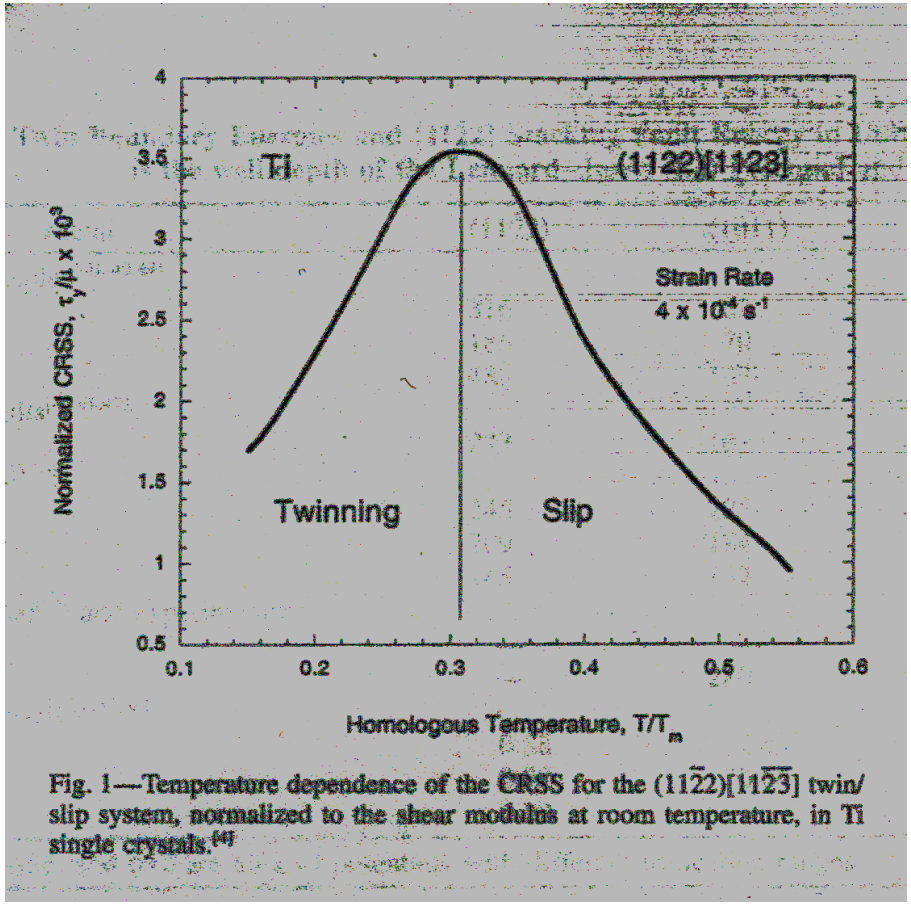

Fig. 1—Temperature dependence of the CRSS for the $(11\bar{2}2)[11\bar{2}\bar{3}]$ twin/slip system, normalized to the shear modulus at room temperature, in Ti single crystals.[4]

Mg Single Crystals

- The available data for temperature dependent CRSS for {1122}<1123> slip in Mg is confusing.
- Yoshinaga and Horiuchi found no evidence of {1122}<1123> slip at elevated temperatures, but identified many types of twins by trace analysis of surface markings.
- Stohr and Poirier [line 8] reported {1122}<1123> slip over a large temperature range by slip trace analysis and TEM observations.
- Line 9 is a rough estimate of CRSS from TEM observations of <c+a> slip dislocations
- Line 10 is for (1122)[1123] slip determined by tension along the [1120] direction

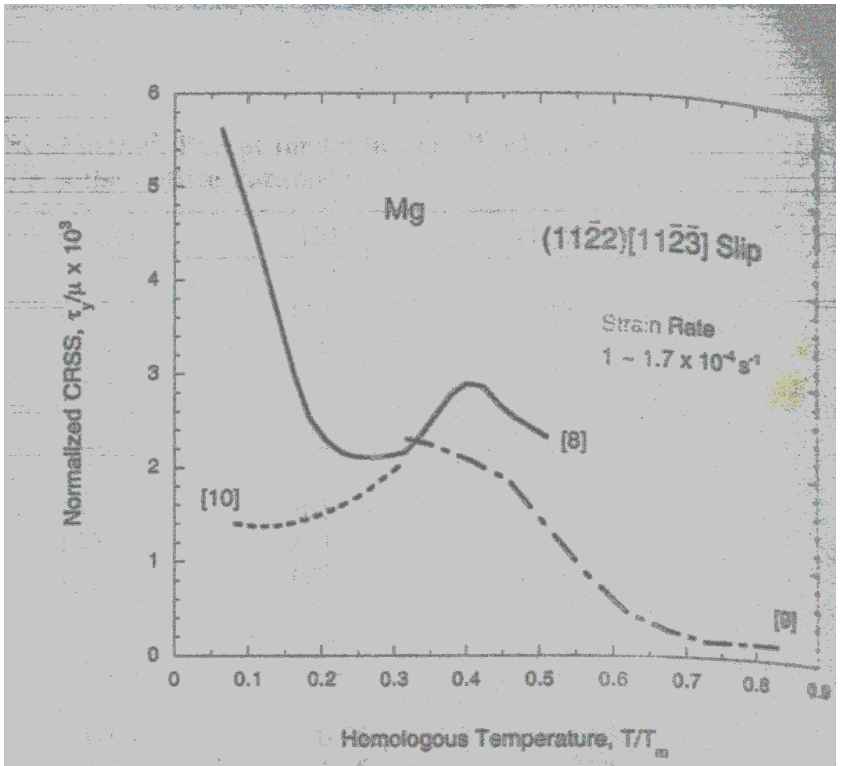

Fig. 2—Temperature dependence of the CRSS for the (11$\bar{2}$2)[11$\bar{2}$3] slip system, normalized to the shear modulus at room temperature, in Mg single crystals.[8,9,10]

Mg Single Crystals

- Plane strain compression was done by Wonsiewicz and Backofen.
  - Compressive strain along the c axis was accomidated by twinning on {1011} and retwinning on {1012}, followed by basel slip in the doubly twinned region.
  - CRSS was not determined for the {1011} twinning, but a strong temperature dependence on the yield stress was observed.

Twin Boundaries and Stacking Faults

- The formation of twins is important to HCP ductility, as demonstrated by the good low temperature ductility of Ti and Zr.
- For atomistic simulations, Yoo, et. al., prefer *ab initio* calculations based on full electronic structure calculations.
  - Many popular atomistic approaches including embeded atom method (EAM) and Finnis-Sinclair (FS) are not very accurate, especially for materials such as Ti and Zr where covalent bonding is important.
  - Some empirical electronic-structure techniques can bridge the gap and provide accurate calculations with less computational burden.
  - However, accurate potentials for most metals is still lacking.

Twin Boundaries and Stacking Faults

Table I. Twin Boundary Energies and {11$\bar{2}$2} Stacking Fault Energy in Units of mJ/m^2, Except for (e) in e/a^2,[34] where e is the well depth of the Lennard–Jones (LJ) Potential and a is the Lattice Parameter

Metal	(11$\bar{2}$2)	(10$\bar{1}$1)	(11$\bar{2}$1)	(10$\bar{1}$2)	(11$\bar{2}$2) SF
(a) First principles[40–42,44]					
Zr	316	82	—	150	305
Mg	186	70	—	114	173
Ti	488	107	—	—	357
(b) EAM results[40,41,42]					
Zr	273	161	—	—	327
(c) FS results[37,38]					
Zr	245	225	169	262	—
Ti	209	184	150	273	—
Mg	145	142	147	188	—
(d) LJ potential[33] and experiment[43]					
lj56	—	—	181	—	—
Ti	—	280	—	—	—
(e) Pair potentials[34,35,36]					
lj56	0.88	2.49	0.69	0.95	1.53
na56	0.92	0.64	0.73	1.15	1.27
ti12	0.89	—	0.89	1.12	—

The lj56, na56, and ti12 are all L–J potentials with different truncation ranges.

- There are only a few results available due to the computational effort of *ab initio* calculations.
- Results indicate that (1012) twins in Zr and Mg are lower in energy than those predicted by empirical potentials.
  - This suggested that observation of the tension twins depend on the formation dynamics rather than the energies.

Twin Boundaries and Stacking Faults

Table I. Twin Boundary Energies and {11$\bar{2}$2} Stacking Fault Energy in Units of mJ/m^2, Except for (e) in ε/a^2,[34] where ε is the well depth of the Lennard–Jones (LJ) Potential and a is the Lattice Parameter

Metal	(11$\bar{2}$2)	(10$\bar{1}$1)	(11$\bar{2}$1)	(10$\bar{1}$2)	(11$\bar{2}$2) SF
(a) First principles[40–42,44]					
Zr	316	82	—	150	305
Mg	186	70	—	114	173
Ti	488	107	—	—	357
(b) EAM results[40,41,42]					
Zr	273	161	—	—	327
(c) FS results[37,38]					
Zr	245	225	169	262	—
Ti	209	184	150	273	—
Mg	145	142	147	188	—
(d) LJ potential[33] and experiment[43]					
lj56	—	—	181	—	—
Ti	—	280	—	—	—
(e) Pair potentials[34,35,36]					
lj56	0.88	2.49	0.69	0.95	1.53
na56	0.92	0.64	0.73	1.15	1.27
ti12	0.89	—	0.89	1.12	—

The lj56, na56, and ti12 are all L–J potentials with different truncation ranges.

- Empirical potentials are given in the table for comparison
  - Note the very low energy for {1011} twin boundary relative to the {1122} boundary for all materials.
  - This is surprising given that this twinning mode is only observed at elevated temperatures
  - These results demonstrate that a simple argument based on classical nucleation theory will not suffice.
- The results also demonstrate a need for accurate calculations. The structures produced by empirical models are close to those from the *ab inito* calculations, but the energies are quite different.

Twin Boundaries and Stacking Faults

Table I. Twin Boundary Energies and {11$\bar{2}$2} Stacking Fault Energy in Units of mJ/m^2, Except for (e) in ε/a^2,[34] where ε is the well depth of the Lennard–Jones (LJ) Potential and a is the Lattice Parameter

Metal	(11$\bar{2}$2)	(10$\bar{1}$1)	(11$\bar{2}$1)	(10$\bar{1}$2)	(11$\bar{2}$2) SF
(a) First principles[40–42,44]					
Zr	316	82	—	150	305
Mg	186	70	—	114	173
Ti	488	107	—	—	357
(b) EAM results[40,41,42]					
Zr	273	161	—	—	327
(c) FS results[37,38]					
Zr	245	225	169	262	—
Ti	209	184	150	273	—
Mg	145	142	147	188	—
(d) LJ potential[33] and experiment[43]					
lj56	—	—	181	—	—
Ti	—	280	—	—	—
(e) Pair potentials[34,35,36]					
lj56	0.88	2.49	0.69	0.95	1.53
na56	0.92	0.64	0.73	1.15	1.27
ti12	0.89	—	0.89	1.12	—

The lj56, na56, and ti12 are all L–J potentials with different truncation ranges.

- Table I also lists the calculated results for the stacking fault on the {1122} plane.
  - This stacking fault has compariable energies to the {1122} twin boundary for Mg, Ti, and Zr.
  - This low energy is due to the local reconstruction of basal planes through the fault, which maintains their close-packed nature.

Twin Nucleation

- Historically there are two main types of twin nucleation mechanisms for HCP metals, based on the homogeneous and heterogeneous nucleation concepts.
- The only experimental data that supports the orginial homogeneous nucleation concept of Orowan was by Price, who observed twin nucleation at re-entrant corners or at specimen grips in dislocation free Zn whiskers.
  - Bell and Cahn prefered the homogeneous nucleation theory for interpreting their data on {1012} twinning in Zn, but only observed twin nucleation after both pyramidal and basel slip had occurred.

Twin Nucleation

- The most potent heterogeneous nucleation site for deformation twinning may be pre-existing dislocations.
- Mendelson suggested the twin formation as a result of nonplanar dissociation of slip dislocations in the HCP lattice.
- The figure illustrates a nonplanar dissociation of Burgers vector b into two glissile partials (p1 and p3) and a sessile partial (p2) that bound two different planar faults.
- An example case is for b=<c+a>, K1=(1121), and η = [1126]

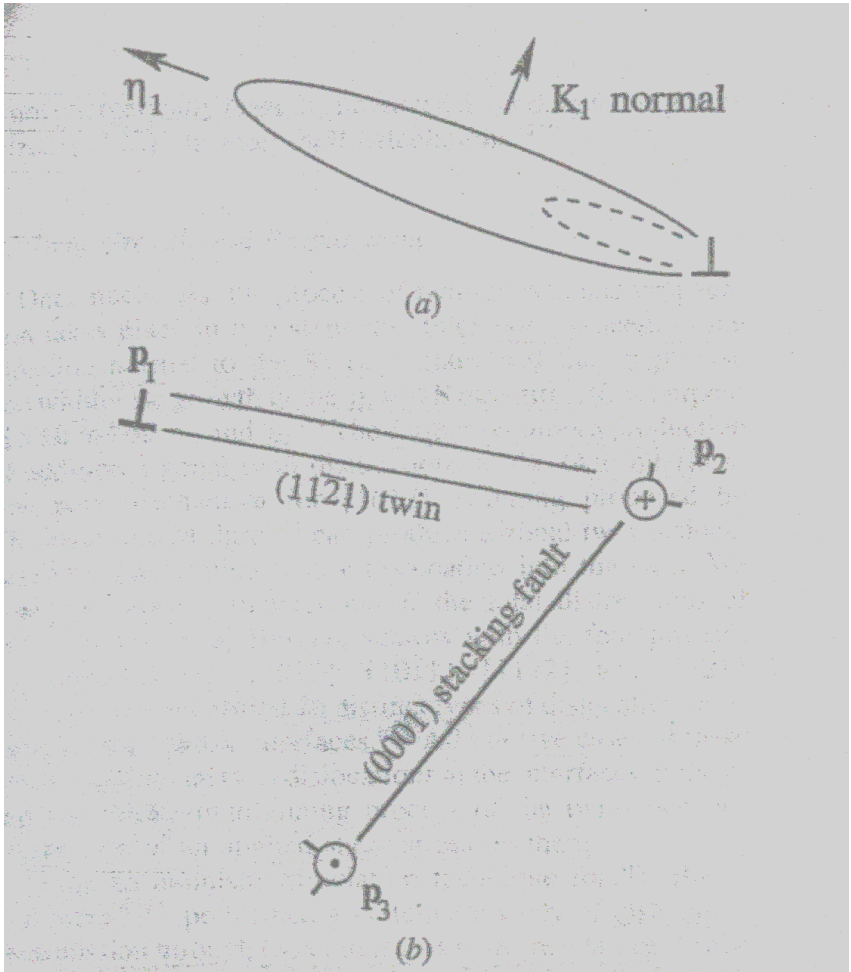

Fig. 3—Schematic descriptions of heterogeneous twin nucleation: (*a*) twin embryo associated with the site of a stress concentration represented by a "super dislocation," and (*b*) generation of twin dislocations as a result of a nonplanar dissociation of an edge dislocation.

Twin Nucleation

- Hirth and Lothe proposed either a true pole or true ratchet mechanism for {1122} twinning.
- The pole is formed by a lattice dislocation of b = <c +a> dissociating into a zonal twin dislocation of b_z~b/4 and three partials with b = (1 +/- f)b/4, where f is a small fraction.
- This dissociation is not energetically feasible according to the generalized {1122} stacking fault calculations.

Twin Growth and Propagation

- Once nucleated the twin growth and propagation takes place in two steps: thickening in the direction normal to K_1 twin plane, and the lengthwise and widthwise growth in the η_1 and S directions
  - The twin thickening requires production of additional zonal twin dislocations at the twin interface
- The pole mechanism for {1012} twinning proposed by Thomson and Millard can produce zonal dislocation by incorporation of a c dislocation into the twin.
- The analysis by Yoo et. al. of the <a>, <c> and <c+a> dislocation interactions with the four primary twin systems identified 26 distinct disloction reactions at the twin-matrix interface.
  - All but five of these cases involve additional twin disloctions at the interface, indicating the thickening/thinning process depends on the sign of the shear stress on them.

Twin Growth and Propagation

- Bacon and Serra used an atomistic simulation technique to systematically study the dislocation transmission through twin interfaces in the hcp lattice.
- They found an unanticipated result while confirming the cross-slip of <a> screw dislocations.
  - The <a> dislocation was absorbed into the {1011} twin interface by the creation of two equal twin dislocations of opposite sign.
- The mobility of the twin dislocations in {1122} boundaries was calculated as marginally higher than those of {1011}, and the twin dislocation with calculated lowest energy and highest mobility for {1011} twinning does not correspond to the mode found in practice.
- This suggests twin nucleation, rather than propagation, may be the mechanism that controls the {1011} mode.

<c+a> Pyramidal Slip

- Grain boundaries are potent sites for initiation of pyramidal slip in polycrystalline materials, and within the grain incoherent twin boundaries are also known as sites for <c+a> dislocations.
- The issue is whether a source produces the total dislocation (likely when the stacking fault energy is high) or a partial dislocation with a strip of stacking fault first and the subsequental generation of another partial dislocation.
- TEM studies by Numakura et. al. in Ti polycrystals found grain boundary sources with the active slip system of {1011}<1123>. Once the glide loop was nucleated the more mobil screw segments cross-sliped from one {1011} plane to another, multiplying the <c+a> disloctions.

<c+a> Pyramidal Slip

- Several groups have observed twins boundaries as sources for <c+a> dislocations in Ti and Mg.
- The <c+a> dislocations were not observed in abundance in the deformed Ti and Mg samples, and where usually observed in conjunction with <a> and <c> dislocations.
- The observed <c+a> dislocations also verified the calculations that indicated that these dislocations are stable in the screw orientation but unstable in the edge orientation.

<c+a> Pyramidal Slip

- One possible source mechanism for <c+a> dislocations is based on the attractive junctions between sessile <c> dislocations and <a> slip dislocations.
- The principle driving force in the junction reaction is from isotropic elastic interaction between two dislocations with mutually perpendicular Burgers vectors.
- It is suggested that the attractive force between a <c> dislocation on the prism plane and the <a> disloction on the basel plane may be sufficiently high to pull the <a> dislocation out of the basel plane.
- For the case of Ti, Zr, and other HCP metals that deform primarily on the prism plane, the proposed model only depends on the last stage (4c) since the formation of an attractive junction on the prism plane is energetically favorable for all hcp metals.

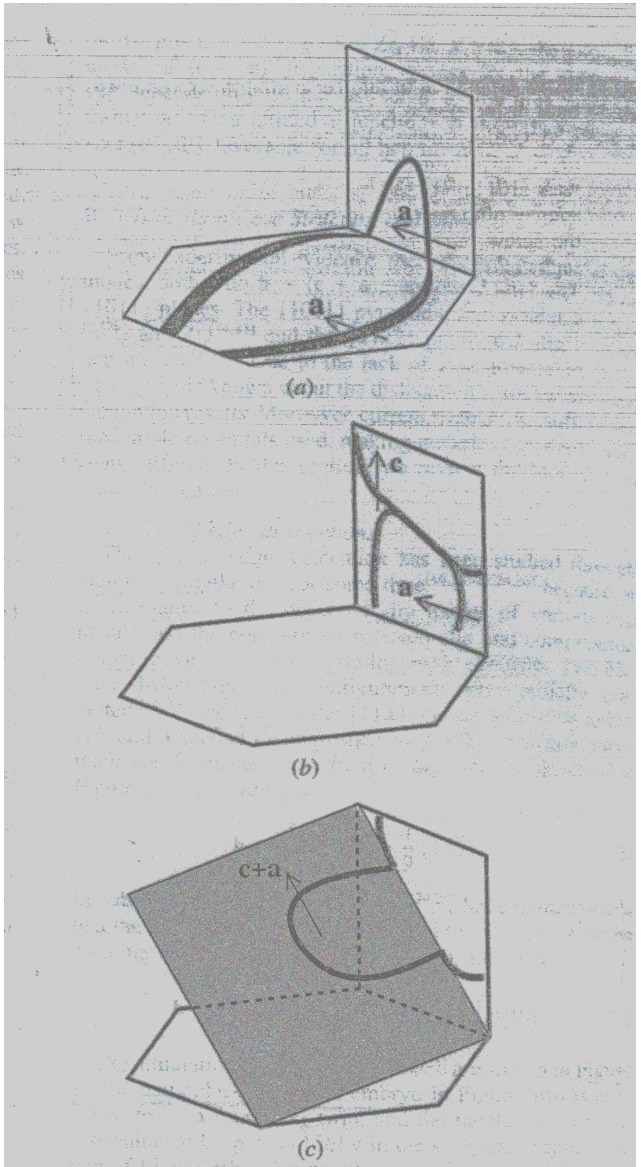

Fig. 4—Evolution of the dislocation source mechanism for the ⟨c + a⟩ pyramidal slip system: (*a*) cross-slip of ⟨a⟩ dislocation, (*b*) formation of ⟨c + a⟩ attractive junction, and (*c*) cross-slip of ⟨c + a⟩ dislocation.

Dislocation Core Structure

- Due to lack of experimental observations, little is known about the dislocation cores except by simulation results.
- The {1122} edge dislocations have been simulated with two different core structures.
- One split on the {1122} plane, and the second nucleated a {1121} twin embryo.

Dislocation Core Structures

- Fig 5 shows the lenticular-shape twin embryo, estimated to be a 4-layer twin terminated by p=[1126].
- This nonplanar sessile dissociation was not observed in earlier simulations due to small simulation geometries.
- The particular type of core structure calculated depended sensitively on the initial position of the core, the interatomic potential, and the relaxation technique.
- This indicates the final structure was not determined by energetic considerations, but instead by initial configuration and subsequent dynamics.

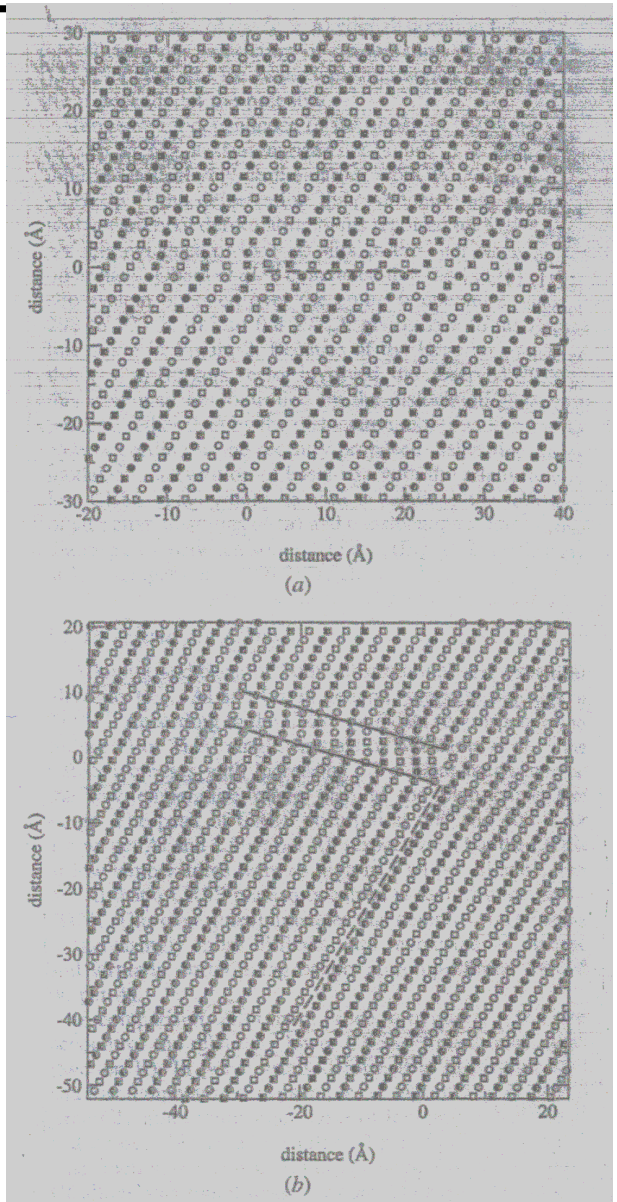

Fig. 5—Two types of dissociation of (c + a) edge dislocation obtained from atomistic simulations: (*a*) planar glissile type and (*b*) nonplanar sessile type.

Dislocation Core Structures

- This figure shows twin growth under applied tensile strain along the c-axis.
- Previous simulations by Liang and Bacon applied only shear strain
- In this case the p_3=[1010]/3 partial is coupled to the strain and extends or contracts the basel plane stacking fault.

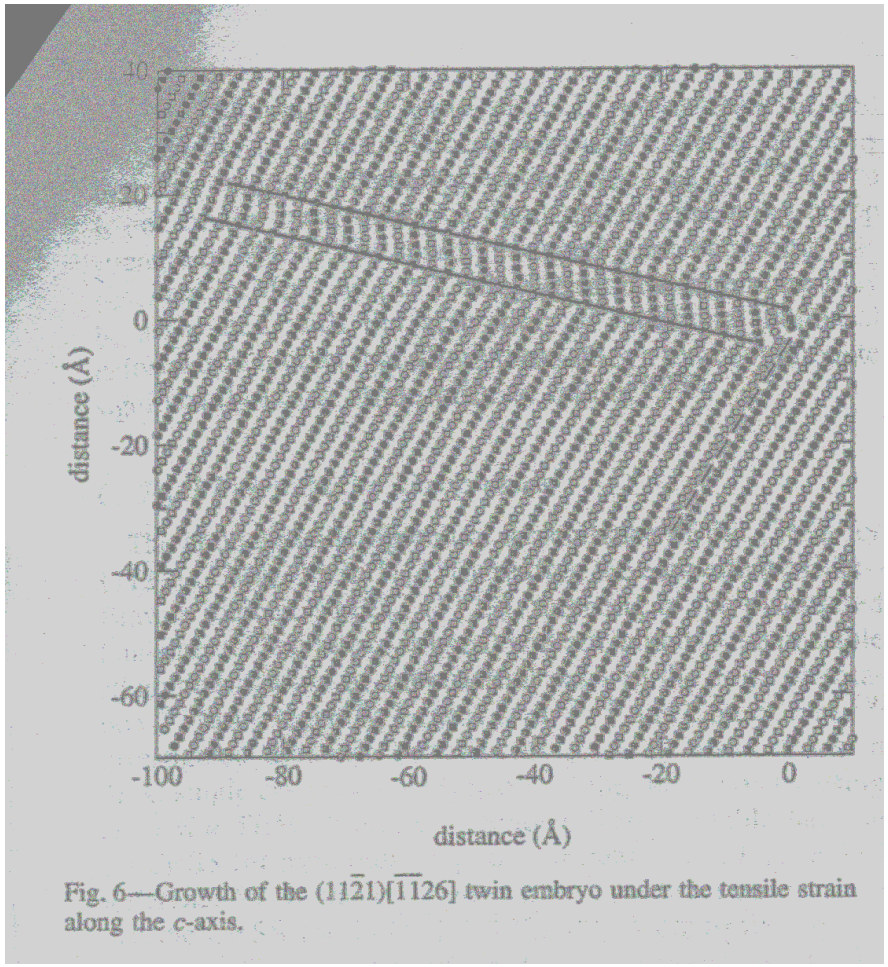

Fig. 6—Growth of the $(11\bar{2}1)[\bar{1}\bar{1}26]$ twin embryo under the tensile strain along the *c*-axis.

Dislocation Core Structures

- This study used interatomic potentials and demonstrated that a dissociated core on the basel plane (Fig5b) had lower energy than split on the (1122) plane (Fig5a), but these potentials do not provide reliable indications of energetics of real materials.
- The planar dissociation in the slip plane corresponds to the observed slip mode in Mg and Be, but the sessile core dissociated in the basal plane is consistant with the twinning in Ti and Zr.

Discussion and Conclusions

Is there CRSS for twinning?

- "Yes" for:
  - {1122} compression twinning in Ti single crystals
  - {1012} tension twinning in Mg 7.7pt Al
- "Difficult to determine" for:
  - {1011} twinning at higher temperatures
- Temperature dependance of CRSS is difficult to determine collectively for <c+a> slip in Mg

Alloying additions suppress twinning in Ti, and in Zr, even with Zr's relatively lower CRSS

Solid-solution alloying of Mg also was found to decrease the CRSS for pyramidal slip.

Disccussion and Conclusions

- The majority of experimental investigations to understand nonbasel deformation modes were conducted in the 1970's.
- The majority of the theoretical analysis to interpret the data was conducted in the 1980's.
- In the past decade theoretical attempts have ben made on material specific prediction of defect structures and energies and the dislocation source mechanisms.
- Further effort is needed experimentally and theoretically at multilevels of length and timescale to better understand the fundamental mechanisms of nonbasel deformation modes and their role in developing a constitutive law of plastic deformation.